Acta Polytechnica CTU Proceedings **1**(1): 103–107, 2014 doi: 10.14311/APP.2014.01.0103

The Formation of Massive Stars: from Herschel to Near-Infrared

Paolo Persi[1], Mauricio Tapia[2]

[1] *Institute for Space Astrophysics and Planetology (IAPS/INAF) Via fosso del cavaliere 100, 00133 Roma, Italy*

[2] *Instituto de Astronomia,UNAM, Apartado Postal 877,Ensenada, Baja California, CP22830, Mexico*

Corresponding author: paolo.persi@iaps.inaf.it

Abstract

We have studied a number of selected high mass star forming regions, including high resolution near-infrared broad- and narrow-band imaging, Herschel (70, 160, 250, 350 and 500 μm) and Spitzer (3.6, 4.5, 5.8 and 8.0 μm) images. The preliminary results of one of this region, IRAS 19388+2357(MOL110) are discussed. In this region a dense core has been detected in the far-infrared, and a young stellar cluster has been found around this core. Combining near-IR data with Spitzer and Herschel photometry we have derived the spectral energy distribution of Mol110. Finally comparing our H_2 and Kc narrow-band images, we have found an H_2 jet in this region.

Keywords: star formation - circumstellar matter - giant molecular clouds - infrared.

1 Introduction

The formation of high-mass stars defined as those with masses greater than 8 M_{sun} is still controversial. One of the crucial problem is to understand if high-mass stars can form through(disk) accretion like low-mass stars. Such stars reach the zero-age main sequence (ZAMS) still undergoing heavy accretion, and their powerful radiation pressure should halt the infalling material, thus inhibiting growth of the stellar mass beyond about 8 M_{sun} (e. g., Palla & Stahler 1993). Recently, various studies have proposed a solution to this problem based on non-spherical accretion and high accretion rates (e. g., McKee & Tan 2003; Bonnell et al. 2004; Kuiper et al. 2010). In addition at difference of low-mass stars, high-mass stars forms in cluster. Therefore the comprehension of the massive star formation process requires good observational knowledge of the star-forming environment and of the evolutionary steps through which OB star formation occurs. This can be made combining observations at different wavelengths from near to far-infrared and millimeter wavelengths. Thanks to the Spitzer and Herschel satellites that operate from the mid-IR to the sub-millimeter it is now possible to have a broad observational coverage of these high mass star formation regions. We have selected a number of these regions reported in Table 1 with typical characteristics of high-mass star formation(i.e. presence of water and methanol maser sources, radio and millimeter emission , ammonia cores, (Molinari et al.1998, Molinari et al. 2000). The type High(H) and Low(L) reported in Table 1 are taken from Molinari et al.1996.. We obtained sub-arcsec resolution near- infrared broad- and narrow-band images of the source of Table 1. These observations are compared with far-IR images from the Herschel Infrared GALactic plane survey (Hi-GAL, Molinari et al. 2010) supplemented with Spitzer/IRAC archive images. The observations are described in Section 2, while in Section 3 we report the preliminary results of IRAS 19388+2357(Mol110). All the results will be discussed in forthcoming papers.

Table 1: Sample of the observed high-mass protostars

Source	Type	IRAS	α(2000)	δ(2000)	D	L
			h m s	° ′ ″	Kpc	$L_\odot$
Mol83	H	18566+0408	18 59 10.0	04 12 15	6.8	1.02×10^5
Mol98	L	19092+0841	19 11 37.4	08 46 30	4.5	9.20×10^5
G45.07+0.13		19110+1045	19 13 22.6	10 50 53	9.7	1.42×10^5
G45.47+0.13			19 14 08.3	11 12 32	6.0	3.80×10^5
Mol110	H	19388+2357	19 40 59.4	24 04 39	4.3	1.48×10^4

1.1 Near-infrared images

Near-infrared images through narrow-band H_2 (λ_o = 2.122 μm, $\Delta\lambda = 0.032\,\mu$m) and $K_{\rm cont}$ ($\lambda_o = 2.270\,\mu$m, $\Delta\lambda = 0.034\,\mu$m) filters, as well as through standard broad-band $JHKs$ filters, were collected on the nights of 2008 July 12 and 14 using the Near Infrared Camera Spectrometer (NICS) attached to the 3.58m Telescopio Nazionale Galileo (TNG) at the Observatorio del Roque de los Muchachos on La Palma island. NICS has a HgCdTe Hawaii 1024 ×1024 array and was used in the SF (small field) configuration with a plate scale of 0.13 arcsec/pixel. In each band, 9 dithered frames spaced by 10 arcsec were taken and coadded, for total on-source integration times of 630 s, 540 s and 360 s for J, H, and Ks, respectively. The total integration time for each of the narrow-band (H_2 and $K_{\rm cont}$) filters was 1170 s. All images were calibrated using photometric standard stars from Hunt et al. (1998) and Persson et al. (1998). The measured FWHM of the point-spread function (PSF) is between 0.6 arcsec and 0.8 arcsec. JHK photometry was obtained using DAOPHOT (Stetson 1987) within IRAF in the standard way, with an aperure of 1 arcsec. For the crowded regions, we used the PSF procedure, also within IRAF.

1.2 HI-GAL images

Hi-Gal is a Herschel open time key-project (Molinari et al.2010) aiming at mapping the Galactic plane with the PACS (70 and 160 μm, Poglitsch et al. 2010) and SPIRE (250, 350, and 500 μm, Griffin et al. 2010) photometers on board the Herschel satellite (Pilbratt et al. 2010). Our target were observed by SPIRE+PACS in parallel mode at a scan speed of 60 arcsec/s. The data were reduced using the Hi-GAL standard pipeline (Traficante et al. 2011). The images have pixel sizes 3.2 arcsec, 4.5 arcsec, 6 arcsec, 8 arcsec, and 11.5 arcsec , at 70, 160, 250, 350, 500 μm respectively. From the images, we performed the source extraction and photometry using the Curvature Threshold Extractor package (CuTEx, Molinari et al. 2011).

1.3 Spitzer/IRAC archive images

Flux-calibrated images of our regions were retrieved from the GLIMPSE (Benjamin et al. 2003, Churchwell et al. 2009) survey taken at 3.6, 4.5, 5.8 and 8 μm with IRAC on board the Spitzer Space Observatory . The flux densities of the mid-infrared counterparts of our sources were extracted from the GLIMPSE Catalogue.

2 IRAS19388+2357(Mol110)

IRAS 19388+2357 is associated with H_2O maser emission (Palla et al. 1991; Brand et al. 1994), a radio source (Hughes & MacLeod 1994; Molinari et al. 1998) and dense molecular gas traced in NH_3 by Molinari et al. (1996) who renamed as Mol110. Methanol maser was also detected from this source (Schutte et al. 1993; Slysh et al. 1994). Zhang et al. (2005) detected a CO outflow. The centroid of their CO emission is approximately 29 arcsec south of the IRAS position. Finally Beltran et al.(2006) detected a dense core at 1.2mm with a mass of 167 M_{sun}. The presence of a UCHII region, of water and methanol maser, confirm that Mol110 is an high-mass star forming region. Figure 1 shows our Ks-band image including the positions of the mentioned sources.

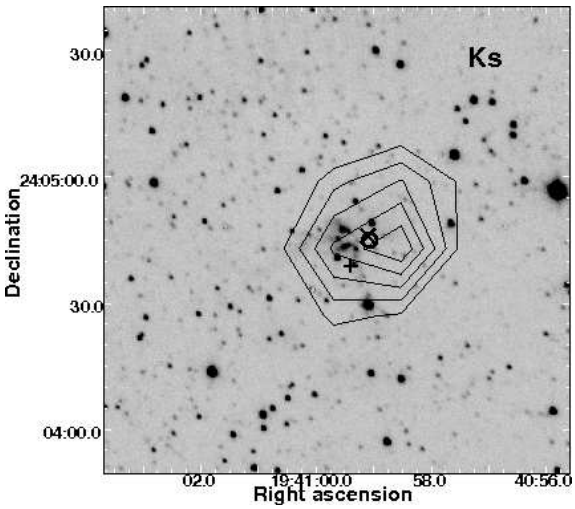

Figure 1: Ks-band image of IRAS19388+23657. The plus indicates the position of the IRAS source, while the open circle and the cross give the positions of the 6cm radio continuum and the MSX source respectively. The contours represent the 1.2mm emission.

A point-like far-infrared sources has been detected in the HI-GAL Herschel images from 70 to 500 μm at the position $\alpha_{2000} = 19^h40^m59.2^s$, $\delta_{2000} = +24^\circ$ 04' 44.9". We have analyzed our JHKs and Spitzer images within an area of approximately 20" × 20" around this position. Figure 2 reports the color-coded JHKs and Spitzer images of this area. Within the Herschel beam we found several very red sources. We have obtained the $JHKs$ photometry of these sources around the Herschel peak position.

From this photometry, we have obtained the $J-H$ versus $H-Ks$ diagram illustrated in Figure 3. More than 14 objects show significant near-infrared excess, suggesting the presence of a young stellar cluster in this region. The positions of these sources are marked in Fig.2 (left panel). At least six of these sources are identified with the mid-IR Spitzer sources (see Fig.2 right panel).

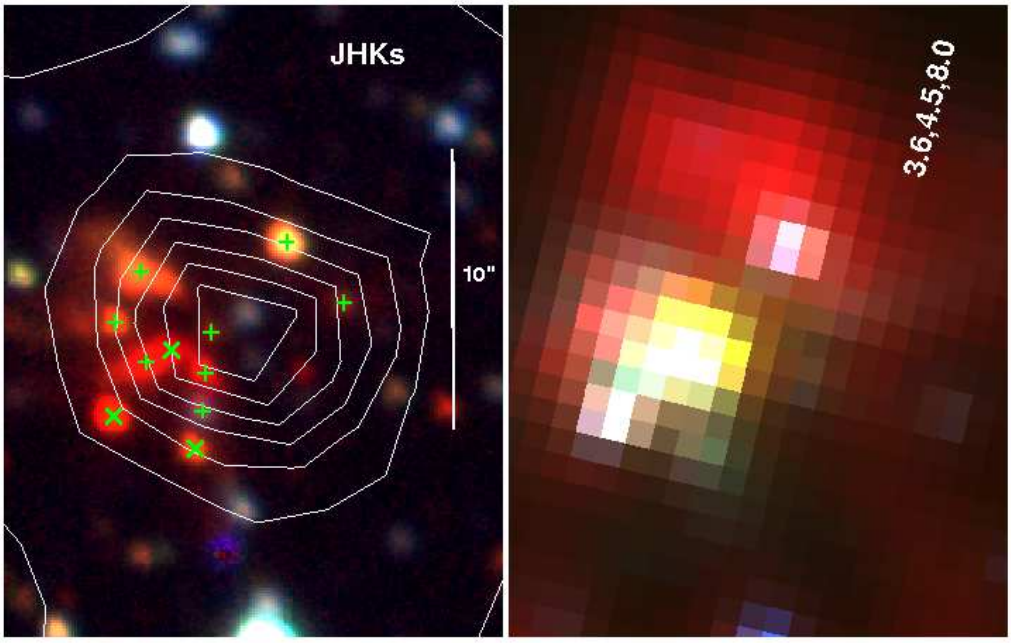

Figure 2: (*Left panel) JHKs* color-coded image of IRAS19388+2375 obtained combining the J (blue), H (green), and Ks (red) individual images The contours show the 70 μm Herschel observation. The symbol (+) marks the positions of the sources with near-IR excess, while the crosses indicate sources not detectect in J but with H-Ks greater than 3(*Right panel)* Color-coded Spitzer image obtained combining the [3.6] (blue), [4.5] (green), and [8.0] μm (red) individual IRAC images. The central position of the two images is $\alpha_{2000} = 19^h40^m59.1^s$, $\delta_{2000} = +24°\ 04'\ 45.4"$. North is at the top and east to the left.

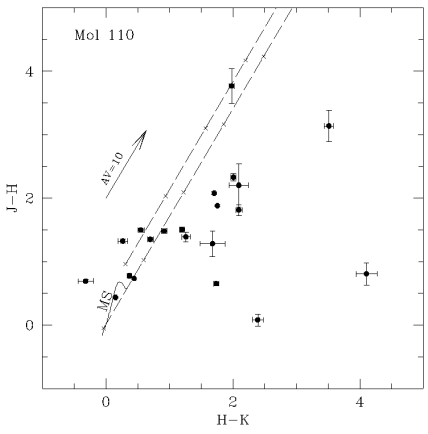

Figure 3: J-H versus H-Ks diagram relative to a region of 20arcsec around the IRAS position.

On the base of the position coincidence, we have identified the far-IR source with a near-IR and Spitzer source. At the same position a source has been detected also with the WISE satellite. Combining data from near-IR to millimeter spectral region we have constructed the spectral energy distribution (SED) of Mol110 reported in Figure 4.

The SED has been fitted with the infalling envelope+disc+central source radiation transfer model described by Robitaille et al. (2006) by using the fitting tool of Robitaille et al. (2007). The parameters of the model that best fit the SED are reported in Table 2.

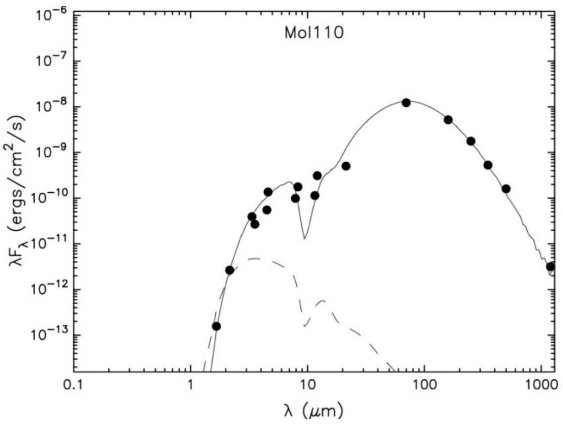

Figure 4: Spectral energy distribution (SED) of Mol 110

The observed luminosity of 1.13 10^4 $L_\odot$ correspond to that of a B1-2 ZAMS star reddened by 50.2 magnitudes of extinction in V.

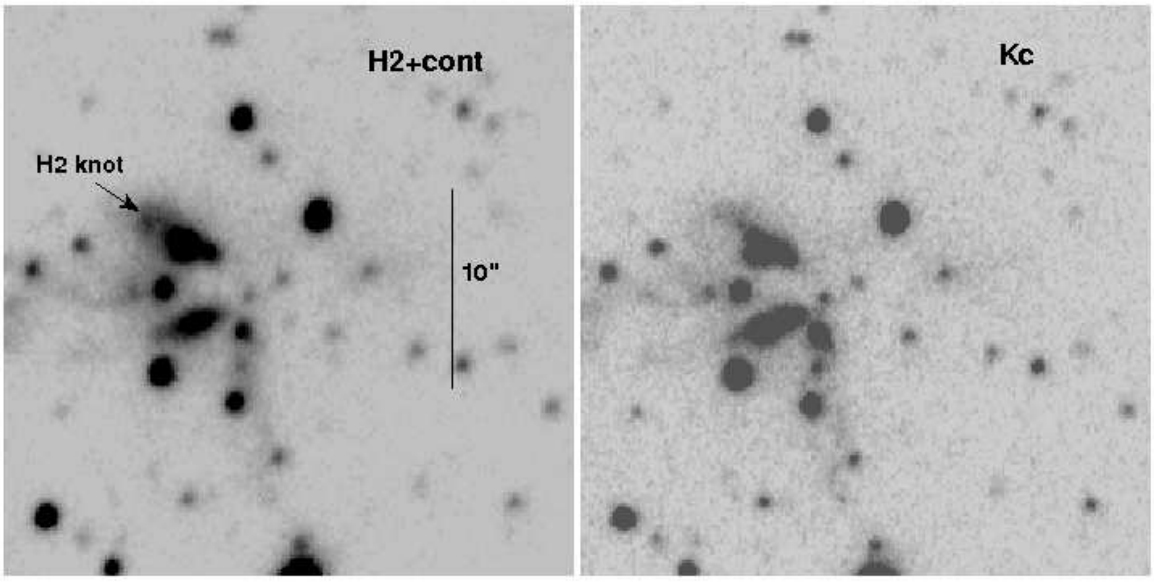

Figure 5: (*Left panel)* H_2 narrow-band image of IRAS 19388+2357. (*Right panel)* Narrow-band Kc image of the same region. North is at the top and east to the left.

Table 2: Physical parameters of Mol 110 derived from the Robitaille et al. (2007) model.

Stella Mass (M_{sun})	12.94
Stellar Temperature (K)	12262
Envelope Accretion Rate (M_{sun}/yr)	3.61 10^{-3}
Envelope Outer Radius (AU)	1.0 10^5
Envelope Cavity Angle (deg)	25.1
Disk Mass (M_{sun})	1.4910^{-1}
Disk Outer Radius (AU)	23.1
Disk Accretion Rate (M_{sun}/yr)	5.18 10^{-6}
A_V	50.2
D(kpc)	4.7
$L_{\rm bol}$	1.13 10^4 $L_\odot$

From the comparison of our narrow-band images centered on the H_2 ($\lambda_o = 2.122\,\mu$m), and nearby continuum $K_{\rm cont}$ ($\lambda_o = 2.270\,\mu$m), we have found an H_2 jet at the position $\alpha_{2000} = 19^h40^m59.7^s$, $\delta_{2000} = +24^\circ$ 04' 49.0" . A nearby source at the position $\alpha_{2000} = 19^h40^m59.5^s$, $\delta_{2000} = +24^\circ$ 04' 47.6" with near-IR excess could be the young stellar object (YSO) driving the observed outflow. This is illustrated in Figure 5. Similar observations obtained by Varricatt et al. (2010) report three different H_2 jets in the region not detected in our images. The positions of these H_2 jets are very far from the CO outflow observed by Zhang et al. (2005), indicating that another YSO is responsible of driving this outflow.

3 Conclusions

In order to understand the physical processes that involve high massive star forming regions, the comparison of observations at different wavelengths from near-IR to millimeter are fundamental. We have here reported an example of this combined analysis including near-IR images, Spitzer data from 3.6 to 8 μm and Herschel images in five bands from 70 to 500 μm, relative to the star forming region IRAS 19388+2357. From this analysis the following conclusions can be made: 1) A very dense and cold core has been detected from the far-IR Herschel images, in proximity of the IRAS source. 2) Within the dense core the near-IR images show the presence of a young stellar cluster of at least 15 members in a radius of 20 arcsec. 3) The far-IR peak has been identified with a bright Spitzer and near-IR source. Combining the photometry from 1.25 μm to 1.2mm, we have derived its spectral energy distribution(SED). The measured total luminosity indicates that the source is a

B1-2 ZAMS with A_V=50.2 4) Finally, the narrow-band image centered on the H_2 line at 2.122 μm shows the presence of an H_2 jet in proximity of the IRAS source.

References

[1] Beltran, M. T., Brand, J., Cesaroni, R., et al.: 2006, A&A, 447, 221

[2] Benjamin, R. A., Churchwell, E., Babler, B. L., et al.: 2003, PASP, 115, 953 doi:10.1086/376696

[3] Bonnell, I. A., Vine, S. G., Bate, M. R.: 2004, MNRAS, 349, 735 doi:10.1111/j.1365-2966.2004.07543.x

[4] Brand J., et al.: 1994, A&AS, 103, 541

[5] Churchwell, E., Babler, B. L., Meade, M. R., et al.: 2009, PASP, 121, 213 doi:10.1086/597811

[6] Griffin, M. J., Abergel, A., Abreu, A., et al.: 2010, A&A, 518, L3

[7] Hughes V. A., MacLeod G. C.: 1994, ApJ, 427, 857

[8] Hunt, L. K., Mannucci, F., Testi, L., et al.: 1998, AJ, 115, 2594

[9] Kuiper, R., Klahr, H., Beuther, H., Henning, T.: 2010, ApJ, 722, 1556 doi:10.1088/0004-637X/722/2/1556

[10] McKee, C. F., Tan, J. C.: 2003, ApJ, 585, 850 doi:10.1086/346149

[11] Molinari S., Brand J., Cesaroni R., Palla F.: 1996, A&A, 308, 573

[12] Molinari, S., Brand, J., Cesaroni, R., Palla, F., Palumbo, G. G. C.: 1998, A&A,336, 339

[13] Molinari, S., Brand, J., Cesaroni, R., Palla, F.: 2000, A&A, 355, 617

[14] Molinari, S., Swuyard, B., Bally, J., et al.: 2010, A&A, 518, L100

[15] Molinari, S., Faustini, F., Schisano, E., et al.: 2011, A&A, 530, A133

[16] Palla F., Brand J., Cesaroni R., Comoretto G., Felli M.: 1991,A&A, 246, 249

[17] Palla, F., Stahler, S. W.: 1993, ApJ, 418, 414

[18] Persson, S. E., Murphy, D. C., Krzeminski, W., et al.: 1998, AJ, 116, 2475

[19] Pilbratt, G. L., Riedinger, J. R., Passvogel, T., et al.: 2010, A&A, 518, L1

[20] Poglitsch, A., Waelkens, C., Geis, N., et al.: 2010, A&A, 518, L2

[21] Robitaille, T. P., Whitney, B. A., Indebetouw, R., et al.: 2006, ApjS, 167, 256

[22] Robitaille, T. P., Whitney, B. A., Indebetouw, R., Wood, K.: 2007, ApjS, 169, 328

[23] Schutte A. J., van der Walt D. J., Gaylard M. J., MacLeord G. C.: 1993, MNRAS, 261, 783

[24] Slysh V. I., Dzura A. M., Valtts I. E., Gerard E.: 1994, A&AS,106, 87

[25] Stetson, P. B.: 1987, PASP, 99, 191

[26] Traficante, A., Calzoletti, L., Veneziani, M., et al.: 2011, MNRAS, 416, 2932

[27] Varricatt, W. P., Davis, C. J., Ramsay, S., Todd, S. P.: 2010, MNRAS, 404, 661
bibitem Zhang Q., Hunter T. R., Brand J., et al.: 2005, ApJ, 625, 864